Structural, electronic, and vibrational properties of liquid and amorphous silicon: Tight-binding molecular-dynamics approach

Eunja Kim and Young Hee Lee
Department of Physics and Semiconductor Physics Research Center, Jeonbuk National University, Jeonju 560-756, Republic of Korea
(Received 14 June 1993)

Liquid and amorphous silicon networks are generated by a tight-binding molecular-dynamics method. The structural, electronic, and vibrational properties are calculated. The generated amorphous silicon networks are mostly fourfold coordinated with dangling bonds (3.2%) and floating bonds (12.5%). The calculated results are in excellent agreements with previous *ab initio* results. These results are further compared to the experimental results and those of other classical models.

I. INTRODUCTION

Amorphous silicon has been extensively studied both theoretically and experimentally not only because of its technological importance but also because of its intrinsic physicals interest. Liquid silicon has also been studied theoretically mostly by introducing classical potentials. Crystalline (c-) and amorphous (a-) silicon (Si) form from covalent bondings while liquid (l-) silicon has metallic character. The melting temperature from c-Si to l-Si is about 1680 K and varies slightly depending on the different experimental processes. The number of nearest-neighbor atoms in a-Si varies from four to more than six, whereas this number in liquid metals is mostly 12. The fact that the coordination number is around $6 \sim 7$ indicates that even in l-Si the silicon atoms have a tendency to form covalent bonds. Although l-Si has been extensively studied theoretically by introducing classical potentials,[1] some physical properties such as phonon frequencies, diffusion constant, and even the contributions from the floating bonds are not well described either qualitatively or quantitatively. In order to overcome these problems with classical potentials, the *ab initio* method for electronic calculations combined with molecular dynamics (MD) has been introduced to describe the ionic motions.[2] Even though this method describes well the experimental results, it is not easily accessible because of the expensive computing time involved in all-electron calculations.

a-Si networks have been generated using classical two- and three-body potentials by Stillinger and Weber (SW).[3] All these models have some dangling bonds and floating bonds. Wooten, Winer, and Wearie (WWW) have generated fourfold-coordinated networks that describe well the structure factor of a-Si from neutron scattering experiment.[4] Car and Parrinello also generated a-Si networks, which are dangling bonds and floating bonds,[5] using an *ab initio* method.

An alternative way to describe all phases of Si structures with both sufficient accuracy and reasonable efficiency is the tight-binding (TB) method combined with MD computer simulation. If one chooses universally fitted TB parameters for the *ab initio* calculations, the efficiency is greatly enhanced compared to the all-electron calculations, and accuracy is automatically achieved. The application of this method for analysis of various structures such as l-Si, point defects in c-Si, and clusters has proved to be very efficient and accurate in comparison to the experimental results.[6] Since only valence electrons are used in the TB method, a large cell can be incorporated in various systems. In this paper, we will adopt the parameterized TBMD introduced by Goodwin, Skinner, and Pettifor[7] to generate l-Si and a-Si. The physical properties of the generated l-Si and a-Si networks will be compared to *ab initio* MD results and the results using the classical model potentials.

II. THEORY

The tight-binding Hamiltonian of a many-electron system involving ionic motion can be written as

$$H = \sum_I \frac{P_I^2}{2m} + \sum_n^{\text{occupied}} \langle \psi_n | H_{\text{TB}} | \psi_n \rangle + \sum_{I<J} \phi(r_{IJ}). \quad (2.1)$$

Here the first term is the kinetic energy of ions and the second term represents the electronic energy of a parametrized TB Hamiltonian. The third term represents a pairwise potential of ion-ion repulsive interactions and also includes the correction for double counting the electron-electron interactions in the second term. In the empirically parametrized TB (ETB) the computing time is greatly reduced by using parameters fitted to the experimental results instead of performing the overlap integrals of electronic interactions everytime. This study adopts the Slater-Koster ETB scheme[8] parametrized by Goodwin, Skinner, and Pettifor.[7] These parameters simply rescale the spatial dependence of hopping integrals of Chadi's scheme,[9] where the spatial dependence of hopping integrals is scaled by the inverse square law. The additional exponential terms in the spatial dependence of hopping integrals reproduce well the total binding energy curve of various phases of Si reproduced from a first principles calculation. The parametrized function is

TABLE I. The parameters constructed by Goodwin, Skinner, and Pettifor (Ref. 7).

$E_s - E_p = 8.295$ eV	
$h_{ss\sigma}(r_0) = -1.82$ eV	$r_0 = 2.35$ Å
$h_{sp\sigma}(r_0) = 1.96$ eV	$r_c = 3.67$ Å
$h_{pp\sigma}(r_0) = -3.06$ eV	$\phi(r_0) = 3.4581$ eV
$h_{pp\pi}(r_0) = -0.87$ eV	

$$h_\alpha(r) = h_\alpha(r_0)\left(\frac{r_0}{r}\right)^2 \exp\left\{2\left[-\left(\frac{r}{r_c}\right)^{6.48}+\left(\frac{r_0}{r_c}\right)^{6.48}\right]\right\}, \tag{2.2}$$

$$\phi_{ij}(r) = \phi(r_0)\left(\frac{r_0}{r}\right)^{4.54} \exp\left\{4.54\left[-\left(\frac{r}{r_c}\right)^{6.48} + \left(\frac{r_0}{r_c}\right)^{6.48}\right]\right\}.$$

Here r_0 is the equilibrium nearest-neighbor distance of the diamond phase and r_c is the potential cutoff distance. The first term represents the spatial dependence of the band structure energy and the second term is the two-body potential energy of ionic repulsive interaction. The index α labels the possible interactions, $ss\sigma$, $sp\sigma$, $pp\sigma$, and $pp\pi$. The relevant parameters are listed in Table I.

The next step is to calculate the forces on each atom. The force is calculated by taking the derivative of the total potential energy with respect to each ionic position,

$$F_I = \ddot{\mathbf{r}}_I = -\frac{\partial E_t(r_{IJ})}{\partial r_I} = -\sum_{J,n}\left\langle \phi_{J,n}\left|\frac{\partial H_{\mathrm{TB}}}{\partial r_I}\right|\phi_{J,n}\right\rangle - \sum_{I>J}\frac{\partial \phi(r_{IJ})}{\partial r_I}, \tag{2.3}$$

where the first term is called the Hellmann-Feynmann force, which is calculated from the orthogonality of the TB wave function, and the second term expresses the pairwise repulsive interaction. This equation is a $3N$-coupled second-order differential equation for given forces from the total potential energy. In principle, the resulting Newtonian equations of motion can be solved from the forces corresponding to given positions and velocities of the ions. To solve the Newton's equations of motion is to predict the future information about the positions, and velocities from present information. This can be done by the predictor-corrector numerical algorithm by Gear.[10]

III. RESULTS AND DISCUSSION

A. Generation of *l*-Si and *a*-Si networks

The constant volume ensemble is used in the whole simulation. The periodic boundary condition along the x, y, and z directions is applied to the supercell of 64 atoms with the density 2.59 g/cm^3. The time step to generate l-Si is 1.08×10^{-15} sec. The potential cutoff distance is 3.2 Å, similar to that of the *ab initio* MD method. In order to generate the l-Si the ideal configuration of the diamond structure is heated for 2 ps at 2000 K, which is above the melting temperature. The temperature is then increased to 2500 K and equilibrated for 2 ps. The temperature is decreased by 200 K and the system is run for 2 ps. This process is repeated down to 1750 K. The system is then equilibrated for a long time at this temperature by repeating the annealing and quenching process until the system is thermally stabilized.

The generation of a-Si networks is more subtle than that of l-Si networks. The fully equilibrated l-Si structure is slowly quenched with a rate of 10^{15} K/sec at every 100 time steps (0.1 ps). When the quenched structure is run with the microcanonical ensemble, the temperature increases. The system is then requenched by the dynamical annealing process as described above. This process is repeated many times (50 ps) until the system is completely quenched to near absolute zero temperature. It should be noted that it is crucial to use well-equilibrated l-Si networks in order to generate good quality a-Si networks. The physical properties are calculated with the equilibrated l-Si and a-Si networks.

B. Structural properties

The generated l- and a-Si are averaged for 2 ps to get the thermal equilibrium properties. Table I represents the parameters used for l-Si. We choose the similar conditions to *ab initio* MD's (Ref. 2) so that we can directly compare the accuracy of our results. The average number of nearest-neighbor atoms is 6.5, in excellent agreement with *ab initio* MD results and experimental values, whereas the classical SW potential result shows large deviations from author to author.[1,3,11–13] The latent heat from c-Si to l-Si is 0.39 eV/atom, a little larger than that from the classical SW potential[3] but closer to the experimental value.[14] This value is not very sensitive to the choice of melting temperature. The melting temperature is different for different models.

Table II represents the corresponding parameters for a-Si. The potential cutoff distance 3.2 Å is used in the generation of a-Si networks. The average number of nearest-neighbor atoms is 4.28 with the cutoff distance 2.75 Å, which is larger than the *ab initio* MD result. This indicates that our model has more floating bonds than theirs. Experimentally this value is less than four, favoring dangling bonds. However, all the theoretical models give this number greater than four. This is due to an unrealistically fast quenching rate that was introduced during the preparation of a-Si networks in the theory.

Shown in Fig. 1 is the radial distribution function of various silicon phases. The c-Si has the bond length at 2.35 Å whereas this value becomes 2.47 and 2.38 Å for l- and a-Si, respectively, in good agreement with previous *ab initio* MD results.[2,5] It is noted that the peak values in a-Si and l-Si vary with the appropriate choice of potential cutoff distance. The distinction between the second and the third nearest-neighbor atoms becomes obscure in

TABLE II. Some physical parameters and results of l-Si.

	TB	*ab initio*[a]	SW[b]	SW[c]	Expt.
Supercell size	64	64	588	216	
Time step (sec)	1.08×10^{-15}	1.3×10^{-16}	1.15×10^{-15}	3.83×10^{-16}	
Density (g/cm^3)	2.59	2.59	2.53	2.53	2.53[d] or 2.59[e]
Cutoff potential (Å)	3.2	3.1	~3.0	4.23	
Coordination number	6.5	6.5	4.89	8.07	6.4[f]
Average nearest-neighbor distance (Å)	2.47	2.46	~2.5	2.56	2.5[f]
$\langle\Theta\rangle \pm \Delta\Theta$ (°)	88.4±37.3		103.9±26.8		
Latent heat (eV/atom)	0.39 (1750 K)		0.32 (1655 K)	0.54	0.47 (1685 K)[g]

[a]Reference 2.
[b]Reference 3.
[c]Reference 1.
[d]Reference 1.
[e]Reference 16.
[f]References 17 and 18.
[g]Reference 15.

a-Si, which is a characteristic of a-Si. Figure 2(a) shows the bond angle distribution function of l- and a-Si with the cutoff distance 2.51 Å. One clearly sees that the a-Si network has a locally covalent bonding nature around 109.5°. With the choice of cutoff distance 3.2 Å, a new peak appears around 50° in l-Si as shown in Fig. 2(b). This can be attributed to the abundant floating bonds in l-Si. It should be noted that l-Si networks from the classical SW potential cannot reproduce the contributions from the floating bonds in the bond angle distribution function, which showed only peaks around 108.3° due to the overestimation of the covalent bondings in the networks. Because of the contribution of the floating bonds, the average bond angle and its deviation are 88.4±37.3° in our network with a cutoff distance of 3.2 Å, which shows large deviations from the 109.5°. This number becomes 106.7±16.3° when the cutoff distance 2.75 Å is used, as shown in Table III, comparable to *ab initio* MD results. This is in contrast with the WWW result which has no dangling bonds and floating bonds. One can see that most deviations result from the contribution of floating bonds. The strain energy which is the total energy difference of c-Si and a-Si is 0.22 eV/atom, giving better agreement with the experimental value over the *ab initio* MD result even though our model has more dangling bonds than the *ab initio* MD model.

Listed in Table IV is the average number of nearest-neighbor atoms of l-Si with a cutoff distance of 3.1 Å,

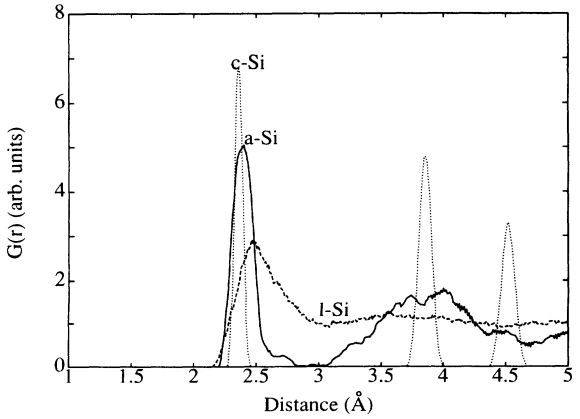

FIG. 1. The radial distribution function of various Si structures. The second and the third peak in a-Si are distinguishable.

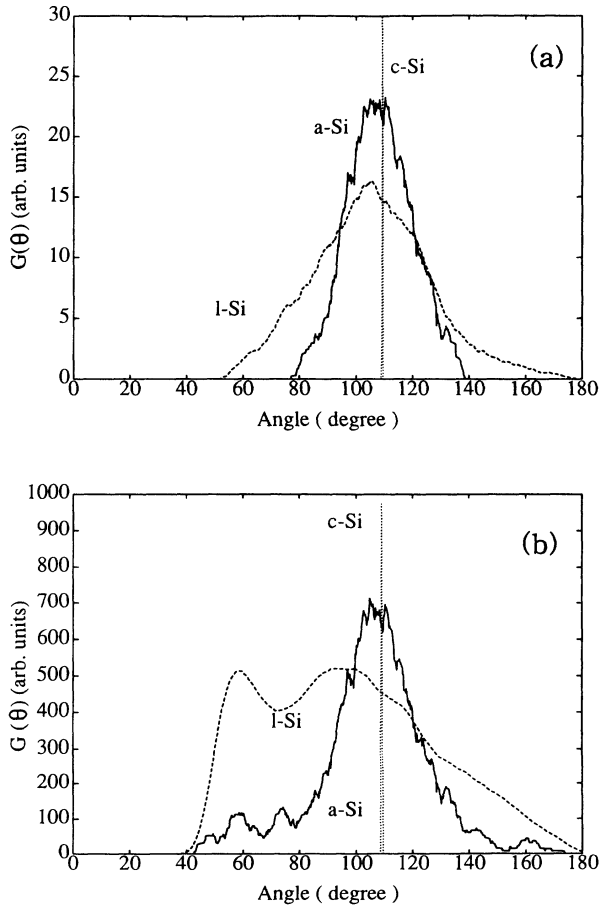

FIG. 2. The bond angle distribution function of various Si structures with cutoff distance (a) 2.51 Å and (b) 3.2 Å.

TABLE III. Some physical parameters and results of a-Si.

	TB	*ab initio*[a]	WWW[b]	SW[c]	Expt.
Quench rate (K/sec)	$\sim 10^{15}$	$\sim 10^{14}$			
Coordination number	4.28	4.03	4.0	$\sim$4.12	3.97[d]
Average nearest-neighbor distance (Å)	2.38	2.39	2.37	$\sim$2.37	2.36[e]
$\langle\Theta\rangle \pm \Delta\Theta$ (°)	106.7±16.3	108.3±15.5	109.5±11	108.3±14.7	109.5±10$\sim$ 11[f]
Strain energy (eV/atom)	$\sim$0.22	$\sim$0.28		0.2$\sim$0.4	$\sim$ 0.18[f]

[a]Reference 5.
[b]Reference 4.
[c]Reference 3.
[d]Reference 19.
[e]References 19 and 20.
[f]Reference 21.

which corresponds to the first minimum point in the radial distribution function. The most probable coordination number is six, which agrees well with the *ab initio* MD result. In general, most metallic liquids have twelve nearest-neighbors atoms. One may expect that the covalent bonding character still exists even in l-Si, whereas this is clearly overestimated in the classical SW potential. Table V lists the average number of nearest-neighbor atoms in a-Si with a cutoff distance of 2.75 Å in our model. All the theoretical models by rapid quenching of l-Si show mostly fourfold-coordinated networks with some amount of dangling and floating bonds. It should be noted that the strain energy of our model is less than that of the *ab initio* MD result, although our model has more dangling and floating bonds, indicating that our a-Si networks are well stabilized.

Figure 3 illustrates typical local bonding structures of l-Si. The local bonding character of l-Si is quite different from that of c-Si, even those of the fourfold-coordinated type, as shown in Fig. 3(a). The bond length ranges from 2.35 to 2.73 Å while the bond angles are 113, 113, 105, and 69°, showing large deviations from the c-Si value of 109.5°. With a neighbor number of five, the bond length and the bond angle scatter in a wider range of values. The average bond length increases with the neighbor number of bondings and some bond lengths are even greater than 3 Å. The bond angles distribute more widely with an increase in the number of neighbor bonds.

Figure 4 illustrates typical local bonding structures of a-Si. The bond lengths with a neighbor number of four are around 2.35 Å, which is quite close to the ideal crystal structure. It is interesting to note that the bond length does not increase significantly with increasing nearest-neighbor number, although the bond angle distribution clearly shows the floating bonding character around 60°. Our networks have a floating bond with six neighboring atoms, which is not seen in the *ab initio* MD model. However, this local bonding is strong with neighboring atoms of all bond lengths smaller than 2.7 Å. We have tried several runs to test the real existence of a floating bond with six neighbors but it always existed. It should be noted that the strain energy is less than that of *ab initio* MD in spite of the existence of floating bonds in our model.

TABLE IV. The average number of nearest-neighbor atoms in l-Si. The cutoff distance 3.1 Å is used in our calculation.

Neighbor number	TB	*ab initio*[a] (%)	SW[b] (%)
3	0.0	0.0	2.3
4	3.1	4.9	29.4
5	21.9	19	47.7
6	43.7	36.4	18.5
7	23.4	23.1	2.1
8	6.3	14.1	0.0
9	1.6	2.5	0.0

[a]Reference 2.
[b]Reference 3.

C. Electronic properties

The electronic structures of various phases can be represented by electronic density of states as shown in Fig. 5. The c-Si clearly shows three distinct peaks of s, p, and s-p orbitals near -10, -7, and -4 eV, respectively. The a-Si still shows the s-like and the p-like orbitals even though the distinction is not as clear as those of c-Si. The gap states near the fermi level are developed due to the dangling bonds, and the conduction band tails are developed, which can be attributed to the contribution of the floating bonds. We see that the electronic bondings still have covalent character in a-Si. This resemblance is completely lost in l-Si. The band gap no longer exists, indicating the metallic character in the electronic structure. Thus one may say that the l-Si has metallic character with some covalent bonding character in the structural properties.

TABLE V. The average number of nearest-neighbor atoms in a-Si. The cutoff distance is 2.75 Å in our calculation.

Neighbor number	TB	*ab initio*[a] (%)	SW[b] (%)
3	3.2	0.2	0.5
4	82.8	96.6	87.8
5	12.5	3.2	11.5
6	1.56	0.0	0.3

[a]Reference 5.
[b]Reference 3.

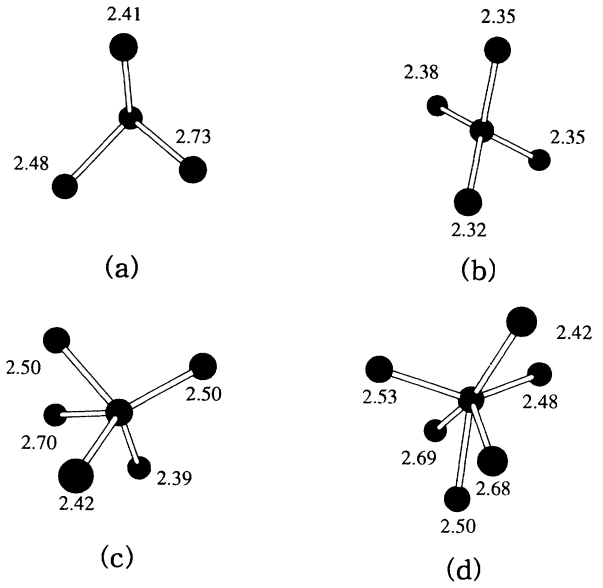

FIG. 3. Typical local bonding structures of l-Si with neighboring number of atoms (a) 4, (b) 5, (c) 6, (d) 7, (e) 8, and (f) 9. The units of bond lengths are in Å.

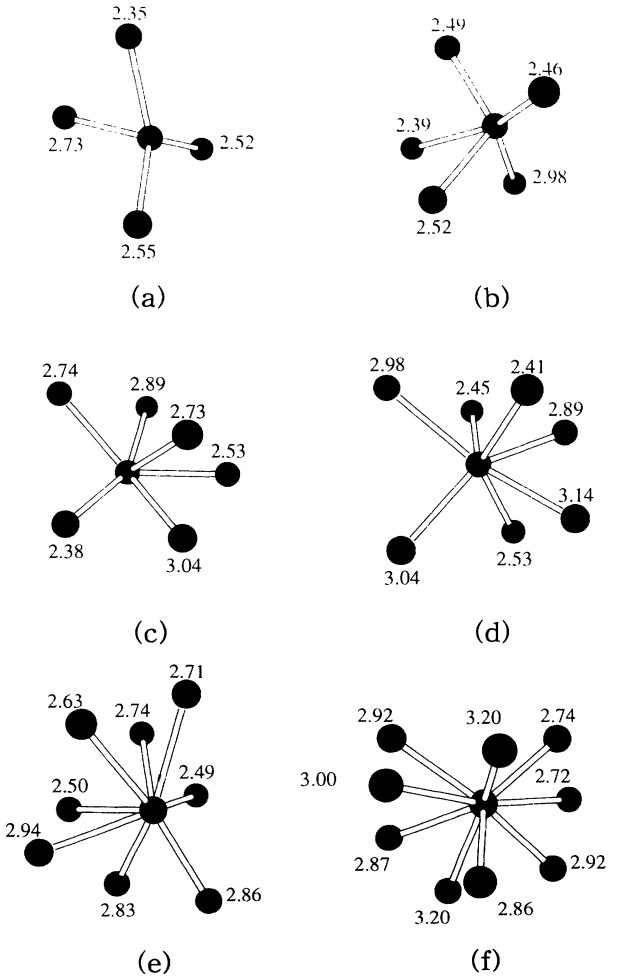

FIG. 4. Typical local bonding structures of a-Si with neighboring number of atoms (a) 3, (b) 4, (c) 5, and (d) 6. The units of bond lengths are in Å.

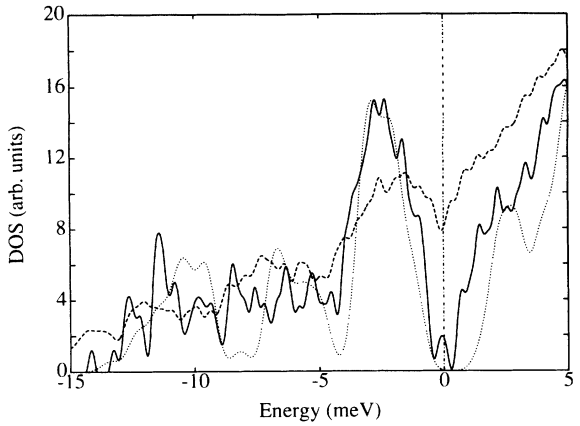

FIG. 5. The electronic density of states of various Si structures; (a) c-Si (dotted line), (b) l-Si (dashed line), (c) a-Si (solid line).

D. Vibrational and dynamical properties

Vibrational properties can be calculated by frozen phonon dynamical matrix calculations assuming harmonic oscillations. In the lattice dynamical calculation, the force constant matrix is constructed by calculating forces on each atom for small displacement x assuming harmonic approximation,

$$F_{i\alpha} = -k_{i\alpha,j\beta}\, x_{j\beta}, \tag{3.1}$$

where $i, j = 1, 2, ..., N$, and $\alpha, \beta = 1, 2, 3$. The normal mode is then determined by solving the matrix equation

$$\det(k_{i\alpha,j\beta}\, x_{j\beta} - m_i\omega^2 x_{i\alpha}) = 0. \tag{3.2}$$

However, in l-Si, the anharmonic effect comes into play. Instead of using the dynamical matrix method, we obtained the normal modes by taking the Fourier transform of velocity-velocity autocorrelation function (VACF),

$$Z(\omega) = \int dt e^{i\omega t} Z(t), \tag{3.3}$$

where the VACF is defined as

$$Z(t) = \sum_{\tau}^{\tau_m} \frac{\langle \mathbf{v}_n(t+\tau)\cdot\mathbf{v}_n(\tau)\rangle}{\langle \mathbf{v}_n(\tau)\cdot\mathbf{v}_n(\tau)\rangle}, \tag{3.4}$$

where the bracket represents the average over the total number of atoms in the system.

Figure 6 shows the phonon density of states (PDOS) of various silicon phases. The c-Si clearly shows four normal modes (TA, LA, LO, TO). The absolute values of these modes agree well with the experimental values. In a-Si the distinction of peak from c-Si is not clear. The TA-like and the TO-like peaks still remain but the LA and the LO modes become blurred because of short range order in a-Si. The PDOS of l-Si is quite different from those of others. No distinct peaks are shown. Instead a broad band over a wide range appears. It is noted that even a zero frequency mode exists, suggesting that the l-Si is very diffusive, as expected. The PDOS of l-Si is

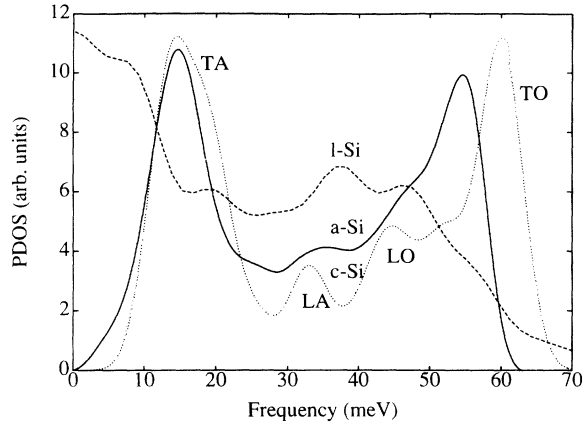

FIG. 6. The phonon density of states of various Si structures.

somewhat different from *ab initio* result in a sense that there is a prominent bump near 50 meV in our model. In order to clarify the difference, we show the VACF in Fig. 7 for different averaging time τ where the dotted and the solid lines are for $\tau = 0.3$ and 1.0 ps, respectively. The inset is the VACF calculated by the *ab initio* MD method. One clearly sees the existence of long tail wiggles in our VACF, whereas that of the *ab initio* MD method does not show the log tail wiggles. The corresponding $Z(\omega)$ are shown in Fig. 8. A bump around 50 meV appears when the total time $t = 1$ ps is used, while this bump becomes smoother when the total time $t = 0.3$ ps is used.[22] If we use the smaller total time in $Z(t)$, we get very smooth $Z(\omega)$ as obtained in the *ab initio* MD model. Therefore, a bump around 50 meV is not fake but real in *l*-Si. The classical SW potential overestimates this bump and less diffusive modes near zero frequency, resulting in the strong covalent bonding character. This was also expected from the less coordination number in classical model. We emphasize that the *l*-Si has a reasonable amount of covalent bonding character even though the electronic structure is metallic.

We also calculate the diffusion constant in *l*-Si. The

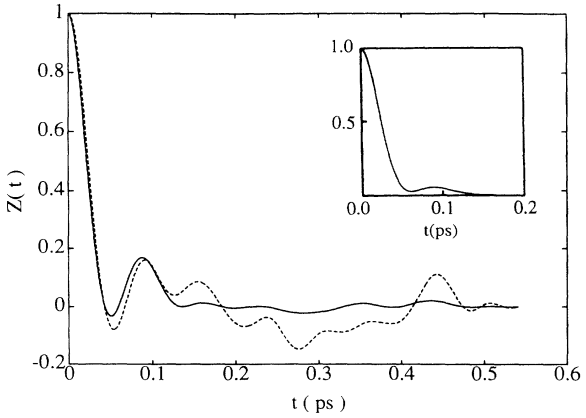

FIG. 7. The velocity-velocity autocorrelation function for different averaging time: (a) $\tau_m = 0.3$ ps for the dotted line, (b) $\tau_m = 1.0$ ps for the solid line. The inset is from the *ab initio* MD model (Ref. 2).

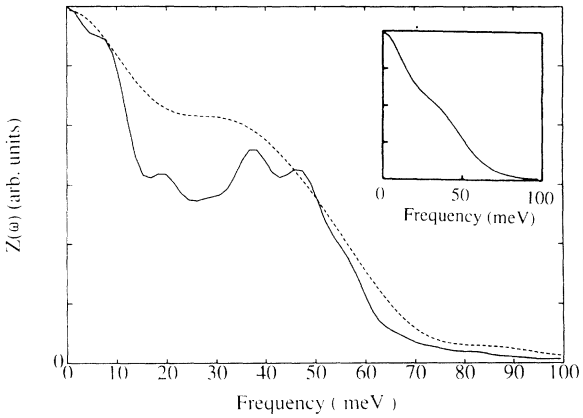

FIG. 8. The Fourier transform of the velocity-velocity autocorrelation function for different times: (a) $t = 0.3$ ps for the dotted line, (b) $t = 1.0$ ps for the solid line. The inset is from the *ab initio* MD model (Ref. 2).

diffusion constant can be calculated by either integrating the VACF or averaging atomic mean displacement,

$$\langle R^2(t)\rangle = \sum_{i=1}^{N}\sum_{\tau=0}^{\tau_m}[\mathbf{R}_i(t+\tau) - \mathbf{R}_i(\tau)]^2, \tag{3.5}$$

where $\mathbf{R}_i(t)$ is the atomic displacement of ith atom at a given time t. The diffusion constant is then calculated by the slope

$$D = \lim_{t\to\infty} \frac{\langle R^2(t)\rangle}{6t}. \tag{3.6}$$

Both methods give similar answers. The calculated diffusion constant at about 1800 K is $\sim 1.98 \times 10^{-4}$ cm^2/sec, as compared to the *ab initio* MD result, 2.26×10^{-4} cm^2/sec, while this value with classical SW potential at 1691 K is 0.94×10^{-4} cm^2/sec. This again reflects the covalent bonding character of our model and others.

IV. CONCLUSION

We have calculated the structural, electronic, vibrational, and dynamical properties of *l*-Si and *a*-Si using parametrized tight-binding molecular-dynamics method. The calculated properties are in excellent agreements with *ab initio* MD results, which clearly proves the efficiency and the accuracy of our method. The *l*-Si networks generated show reasonable amounts of covalent bonding character, although the electronic structure is metallic. The *a*-Si networks generated are mostly fourfold-coordinated with dangling bonds (3.2%) and floating bonds (12.5%). This model will be used for the defects in *a*-Si in the future.

ACKNOWLEDGMENT

This work was supported by the Korea Science and Engineering Foundation (KOSEF) through the Semiconductor Physics Research Center (SPRC) at Jeonbuk National University.

[1] F. H. Stillinger and T. A. Weber, Phys. Rev. B **31**, 5262 (1985).
[2] I. Stich, R. Car, and M. Parrinello, Phys. Rev. B **44**, 4262 (1991).
[3] W. D. Luedtke and U. Landman, Phys. Rev. B **37**, 4656 (1988).
[4] F. Wooten, K. Winer, and D. Wearie, Phys. Rev. Lett. **54**, 1392 (1985).
[5] I. Stich, R. Car, and M. Parrinello, Phys. Rev. Lett. **60**, 204 (1988); Phys. Rev. B **44**, 11 092 (1991).
[6] C. Z. Wang, C. T. Chan, and K. M. Ho, Phys. Rev. B **45**, 12 227 (1992); E. G. Song, E. Kim, and Y. H. Lee, Phys. Rev. B **48**, 1486 (1993); I. H. Lee, K. J. Chang, and Y. H. Lee (unpublished).
[7] L. Goodwin, A. J. Skinner, and D. G. Pettifor, Europhys. Lett. **9**, 701 (1989).
[8] J. C. Slater and G. F. Koster, Phys. Rev. B **94**, 1498 (1954).
[9] D. J. Chadi, Phys. Rev. Lett. **41**, 1062 (1978); Phys. Rev. B **29**, 785 (1984).
[10] C. W. Gear, in *Numerical Initial Value Problems in Ordinary Differential Equations* (Prentice-Hall, Englewood Cliffs, NJ, 1971).
[11] J. Q. Broughton and X. P. Li, Phys. Rev. B **35**, 9120 (1987).
[12] M. D. Kluge, J. D. Ray, and A. Rahman, Phys. Rev. B **36**, 4234 (1987).
[13] W. D. Luedtke and U. Landman, Phys. Rev. B **40**, 1164 (1989).
[14] K.-H. Hellwege and U. Madelung, *Numerical Data and Functional Relationship in Science and Technology*, Landolt-Börnstein, New Series, Group III, Vol. 17 (Springer-Verlag, Berlin, 1982).
[15] A. R. Ubbelohde, *The Molten State of Matter* (Wiley, New York, 1978), p. 239.
[16] Y. Waseda, *The Structure of Non-Crystalline Materials; Liquids and Amorphous Solids* (McGraw-Hill, New York, 1980).
[17] Y. Waseda and K. Kuzuki, Z. Phys. B **20**, 339 (1975).
[18] J. P. Gabathuler and S. Steeb, Z. Naturforsch. Teil A **34**, 1314 (1979).
[19] M. Benfatto, C. R. Natoli, and A. Filipponi, Phys. Rev. B **39**, 5527 (1989); A. Filipponi, F. Evangelisti, M. Benfatto, Mobilio, and C. R. Natoli, *ibid.* **40**, 9636 (1989).
[20] J. Forther and J. S. Lannin, Phys. Rev. B **39**, 5527 (1989).
[21] S. Rooada, Ph. D. thesis, FOM Amsterdam, 1989; W. C. Sinke, S. Roorda, and F. W. Saris, J. Mater. Res. **3**, 120 (1988); S. Roorda, S Doorn, W. C. Sinke, R. M. L. O. Scholte, and E. Van Loenen, Phys. Rev. Lett. **62**, 1880 (1989).
[22] The maximum average time τ_m is the same as total time which is used for the Fourier transform. See, for instance, W. H. Press *et al.*, *Numerical Recipes* (Cambridge University Press, Cambridge, 1989), p. 381.